Available online at www.sciencedirect.com
SCIENCE DIRECT®

Journal of the European Ceramic Society 24 (2004) 1497–1500

www.elsevier.com/locate/jeurceramsoc

Characteristic dielectric behavior and crystal structure of $(1-x)Pb(Yb_{1/2}Ta_{1/2})O_3-xPb(Fe_{1/2}Ta_{1/2})O_3$ at $0.00 \leqslant x \leqslant 0.10$

Sang Chul Youn, Woong Kil Choo*

Department of Materials Science and Engineering, Korea Advanced Institute of Science and Technology, 373-1 Gusong-Dong, Yusong-Gu, Taejon 305-701, South Korea

Abstract

The crystal structure and the phase transition of $(1-x)Pb(Yb_{1/2}Ta_{1/2})O_3-xPb(Fe_{1/2}Ta_{1/2})O_3$ solid solutions in the antiferroelectric range for $0 \leqslant x \leqslant 0.10$ have been studied by the dielectric constant measurements, E–P hysteresis measurements, X-ray diffraction and transmission electron microscopy (TEM). In the composition region $x \leqslant 0.10$, the dielectric dispersion which is the secondary phase transition point of pure PYT remains and it exhibits slim loop which means that the solid solution is ferroelectric at low temperatures. From the X-ray diffraction analysis of the superlattice structure of $(1-x)$PYT$-x$PFT solid solutions, it is found that there are no basic structural changes as x increases up to $x = 0.10$. But in the TEM analysis, the antiferroelectric phase is shown to coexist with the ferroelectric phase below the secondary phase transition temperature. In the selected area diffraction pattern (SADP), an intermediate incommensurate phase is observed.

Keywords: $(1-x)$PYT$-x$PFT; Dielectric properties; Ferroelectric properties; Perovskites

1. Introduction

Lead-based complex perovskites with the general formula of $Pb(B'B'')O_3$ show several types of interesting dielectric behavior depending on the degree of the B-site cation ordering. Their dielectric behavior is dependent on the chemical composition and geometrical distribution of B-site cations in the perovskite lattice.[1]

$Pb(Yb_{1/2}Ta_{1/2})O_3$ (PYT) is a highly ordered complex perovskite.[2,3] This compound exhibits a sharp first order phase transition. In addition, PYT undergoes a secondary phase transition below the primary transition temperature. The primary phase paraelectric (PE)–antiferroelectric (AFE) transition occurs at 310 °C, and the secondary AFE-ferroelectric (FE) phase transition occurs near 186 °C.[2] This peculiar transition pattern is very similar to that of highly ordered $PbCo_{1/2}W_{1/2}O_3$ (PCW) that also has two successive phase transitions (PE–AFE–FE).[4,5] Particularly, PCW is antiferroelectric at room temperature.[6] X-ray and transmission electron microscopy (TEM) studied on highly ordered PCW have revealed the existence of an incommensurate phase.[6–8]

In the present study, $(1-x)$PYT$-x$PFT solid solutions were examined by the dielectric constant and E–P hysteresis measurements and by X-ray diffraction (XRD). For the microstructure study at secondary transition, transmission electron microscopy (TEM) is executed at room temperature.

2. Experimental

Ceramic $(1-x)$PYT$-x$PFT were obtained, starting from a mixture of stoichiometric amounts of high purity (99.9%) PbO, Yb_2O_3, Ta_2O_5 and Fe_2O_3 powders. The mixture was ball-milled in acetone and then calcined at 900–950 °C for 2 h. The calcined powders were ground and shaped into pellets. The pellets were isostatically cold pressed and then sintered at 950–1000 °C for 1 h. The sintered ceramics were cut into thin discs and electroded with silver paste before the dielectric measurements.

The dielectric constants were measured at several frequencies, 1, 10, 100 K and 1 MHz, using a Hewlett-Packard 4194A Impedance/Gain Phase Analyser. During measurements, the samples were heated at a constant rate of 3 °C/min. X-ray diffraction measurements were carried out on a two-circle X-ray diffractometer (D/max-RB) using the Cu-K_α radiation operated at

* Corresponding author. Tel.: +82-42-869-4123-4253; fax: +82-42-869-4123-4273.

0955-2219/$ - see front matter © 2003 Elsevier Ltd. All rights reserved.
doi:10.1016/S0955-2219(03)00559-4

40 kV and 100 mA. The X-ray diffraction patterns were scanned continuously in 2θ in steps of 0.02 degrees. TEM specimens were thinned to 3 mm disks that were mechanically polished to 80 μm thickness. The center parts of these disks were then further thinned by a dimpler to 10 μm thickness, and then argon ion milled to perforation. TEM studies were performed on a Phillips CM20/T microscope operating at the accelerating voltage of 200 kV.

3. Results and discussion

3.1. Dielectric properties

Fig. 1 illustrates the temperature dependence of the dielectric constant(ε') of $(1-x)$PYT$-x$PFT solid solutions($x \leqslant 0.10$) at various frequencies on the heating. In this composition range, the solid solution undergoes two successive phase transition: a primary PE–AFE and a secondary AFE–FE phase.

The dielectric constant maximum of the primary transition slowly decreases with the Fe ion substitution. On the other hand, the phase transition temperature increases with the Fe ion substitution.

We would like to point out that there is a secondary AFE–FE phase transition in $(1-x)$PYT$-x$PFT. The secondary phase transition is diffuse and depends on the frequency similar to a dielectric relaxor. The dielectric constant maximum of the secondary transition shows the decreasing tendency like the primary transition. At $x=0.10$, this secondary transition is so diffuse that it becomes impossible to distinguish it from the dielectric constant vs temperature curve.

We then had to determine whether the secondary transition of the solid solution is indeed an AFE–FE transition. This can be indicated by E–P hysteresis measurement. Fig. 2 illustrates the E–P hysteresis curves of $(1-x)$PYT$-x$PFT ($x \leqslant 0.10$) at different temperatures. The results show slim loops. It is evident that a weak FE phase or an AFE/FE phase mixture exists below the secondary transition temperature in these solid solutions.

As the temperature increases, the spontaneous polarization, P_S and the coercive field, E_C both disappear and this proves the existence of an AFE phase above the secondary transition temperature but below the primary transition. Also the hysteresis becomes slimmer as Fe ion concentration increases. This means that the AFE phase is gradually stabilized by PFT addition.

3.2. X-ray diffraction pattern

X-ray diffraction patterns for the $(1-x)$PYT$-x$PFT solid solutions are shown in Fig. 3. The diffraction pattern may be analyzed in reference to that of AFE $PbYb_{1/2}Nb_{1/2}O_3$.[9] The diffraction patterns are superposed of two types of superlattice reflection lines. The first set represents the ordering of B-site atoms of which reflection intensity depends on the difference of atomic scattering factor between the B-site cations. The second represents the antiparallel Pb cation shift. As previously reported,[2,3] pure PYT ($x=0.0$) shows monoclinic distortions from the perovskite crystal structure. For pure PYT, two types of superlattice reflections are clearly observed.[10] The B-site ordering superlattice reflections are still present up to $x=0.10$ on Fe substitution. Although the variation of the secondary transition is

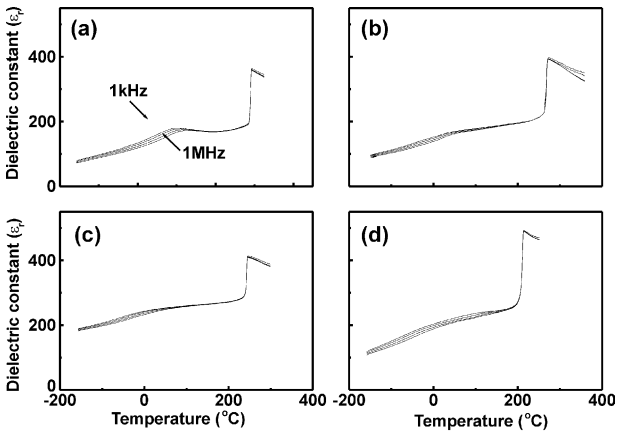

Fig. 1. Temperature dependence of the real dielectric constant for $(1-x)$PYT$-x$PFT: (a) $x=0.02$; (b) $x=0.05$; (c) $x=0.07$; (d) $x=0.10$.

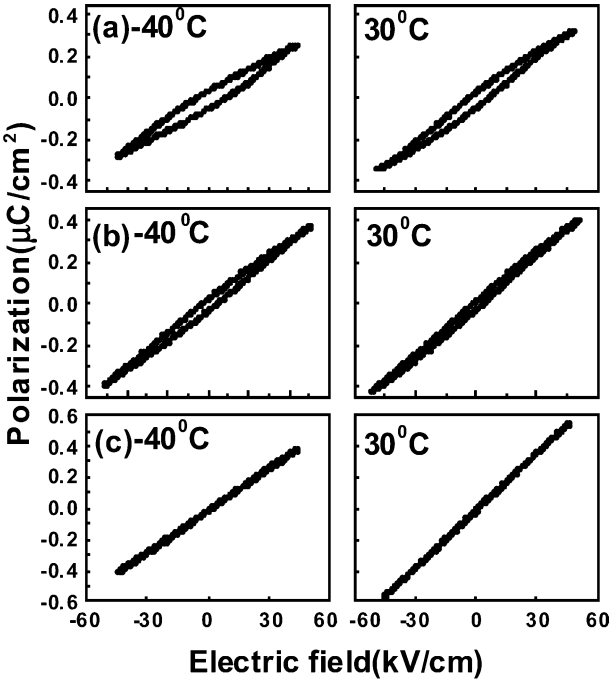

Fig. 2. E–P hysteresis loop as a function of PFT concentration x and temperature for: (a) $x=0.02$; (b) $x=0.05$; and (c) $x=0.10$.

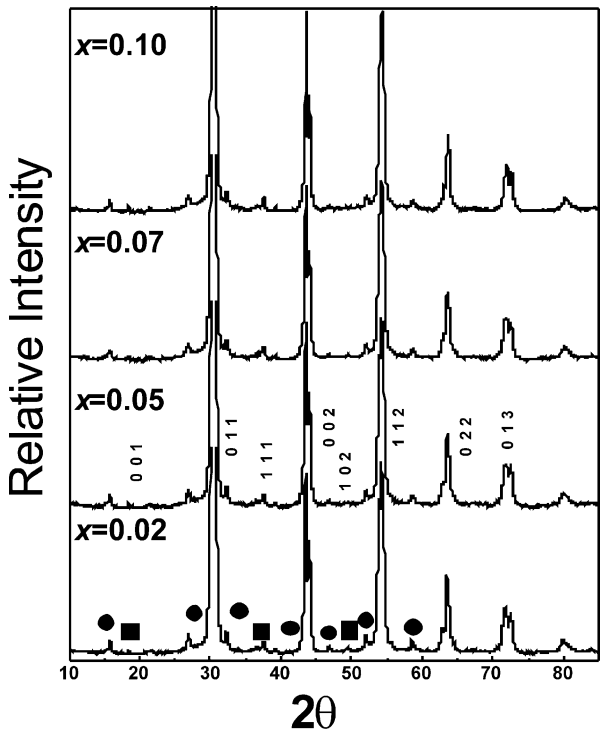

Fig. 3. X-ray diffraction patterns of the $(1-x)$PYT$-x$PFT system at room temperature.

observed on Fe substitution below $x=0.10$, there is no such peak and structural variation beyond their composition.

Considering the $(1-x)Pb(Yb_{1/2}Ta_{1/2})O_3-xPb(Fe_{1/2}Ta_{1/2})O_3$ dielectric constant curve and the E–P hysteresis, the AFE phase becomes more stabilized with the increasing Fe ion concentration. However, any structural change on the Fe ion substitution is not detected on the XRD patterns.

3.3. TEM investigation

Fig. 4 shows the selected area diffraction patterns (SADPs) for the compositions $x=0.02$, 0.05, 0.07 and 0.10. They clearly show the AFE spots. Kim and Choo[11] reported that all the pure PYT spots have the rational ratio interval. But as the Fe ion concentration is increased, it is found that the superlattice spots of the solid solution which were equally spaced along the [110] direction are moved. The superlattice spots of $(1-x)$PYT$-x$PFT are arranged in irrational-ratio along the [110] direction as shown in Fig. 4. The reported dielectric constant curve and E–P hysteresis loop of PCW are similar to the current solid solutions[12,13] and it has also been reported that the AFE phase crystal structure of PCW is incommensurate at room temperature.[5]

As mentioned before, there is no macrostructural change in $(1-x)$PYT$-x$PFT solid solution below

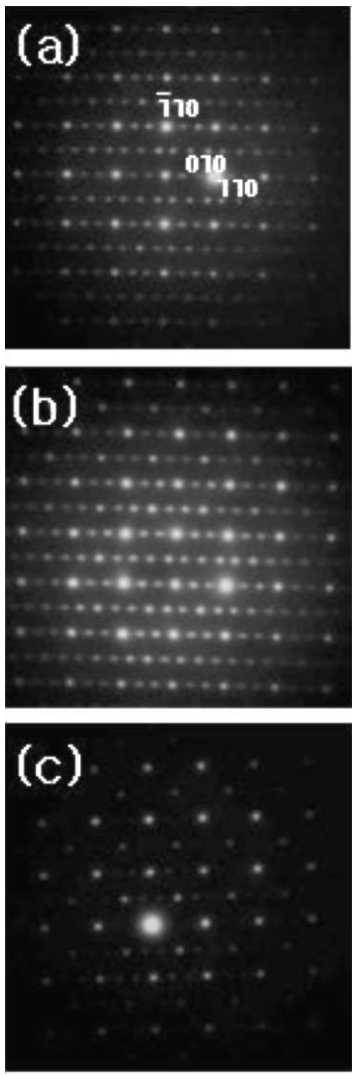

Fig. 4. Selected area diffraction patterns of the $(1-x)$PYT$-x$PFT: (a) $x=0.02$; (b) $x=0.05$; and (c) $x=0.10$.

$x=0.10$. From the PCW–PYT comparison, it is inferred that the AFE phase stabilization is correlated with the incommensurate lattice modulation.

4. Conclusions

The $(1-x)$PYT$-x$PFT solid solution was investigated by the dielectric constant measurement, X-ray and TEM measurements. At $x\leqslant 0.10$, two successive phase transitions are clearly identified by the dielectric measurement. In this region, the $(1-x)$PYT$-x$PFT solid solution is FE ; as verified by E–P hysteresis measurement. As the Fe ion concentration is increased, the AFE phase of this solution system is gradually stabilized. The SADPs of the $(1-x)$PYT$-x$PFT solution show the evidence of incommensuration in contrast to the commensurate SADP of pure PYT.

Acknowledgements

This work was supported by the Korea Science and Engineering Foundation through the Research Center for Advanced Magnetic Materials at Chungnam National University.

References

1. Randall, C. A. and Bhalla, A. S., Nanostructural-property relation in complex lead perovskite. *Jpn. J. Appl. Phys.*, 1990, **29**, 327–333.
2. Yasuda, N. and Konda, J., Successive paraelectric-antiferroelectric phase transitions in highly ordered perovskite lead ytterbium tantalite. *Appl. Phys. Lett.*, 1993, **62**, 535–537.
3. Yasuda, N. and Konda, J., Ferroelectric in highly ordered perovskite lead ytterbium tantalite. *Ferroelectrics*, 1994, **158**, 405–410.
4. Hachiga, T., Fujimoto, S. and Yasuda, N., Pressure and temperature dependence of dielectric properties $Pb(Co_{1/2}W_{1/2})O_3$. *Jpn. J. Appl. Phys.*, 1985, **24**(3), 239–241.
5. Bonin, M., Paciorek, W., Schenk, K. J. and Chapuis, G., X-ray study of and structural approach to the incommensurate perovskite Pb_2CoWO_6. *Acta Cryst. B*, 1995, **51**, 48–54.
6. Randall, C. A., Bhalla, A. S., Shrout, T. R. and Cross, L. E., Classification and consequences of complex lead perovskite ferroelectrics with regard to B-site cation order. *J. Mater. Res.*, 1990, **5**, 829–834.
7. Randall, C. A., Markgraf, S. A., Bhalla, A. S. and Baba-Kishi, K., Incommensurate structures in highly ordered complex perovskites $Pb(Co_{1/2}W_{1/2})O_3$ and $Pb(Sc_{1/2}Ta_{1/2})O_3$. *Phys. Rev., B*, 1989, **40**, 413–416.
8. Baba-Kishi, K. Z. and Barber, D. J., Transmission electron microscope studies of phase transitions in single crystals and ceramics of ferroelectric $Pb(Sc_{1/2}Ta_{1/2})O_3$. *J. Appl. Cryst.*, 1990, **23**, 43–54.
9. Kwon, J. R. and Choo, W. K., The antiferroelectric crystal structure of the highly ordered complex perovskite $Pb(Yb_{1/2}Nb_{1/2})O_3$. *J. Phys.: Condens. Matter*, 1991, **3**, 2147–2155.
10. Park, S. B. and Choo, W. K., Structural and dielectric studies of the phase transitions in $Pb(Yb_{1/2}Ta_{1/2})O_3$-$PbTiO_3$ ceramics. *Jpn. J. Appl. Phys.*, 2000, **39**, 5560–5564.
11. Kim, H. J. and Choo, W. K., The dielectric properties and phase transition of (1-x)$Pb(Yb_{1/2}Ta_{1/2})O_3$-x $Pb(Yb_{1/2}Nb_{1/2})O_3$. *Jpn. J. Appl. Phys.*, 2001, **40**, 5668–5670.
12. Xu, Z., Vieland, D. and Payne, D. A., An incommensurate–commensurate phase transformation in antiferroelectric tin-modified lead zirconate titanate. *J. Mater. Res.*, 1995, **10**, 453–460.
13. Sciau, Ph., Krusche, K., Buffat, P.-A. and Schmid, H., Electron diffraction study of the Pb_2CoWO_6 phases. *Ferroelectrics*, 1990, **107**, 235.